Journal of Applied Mechanics and Technical Physics, Vol. 41, No. 5, 2000

SHOCK-WAVE STRUCTURE IN THE NEAR ZONE UPON EXPLOSION OF SPATIAL CHARGES IN AIR

A. V. Pinaev, V. T. Kuzavov, and V. K. Kedrinskii

UDC 534.222.2

Profiles and values of pressure in shock waves are determined for the case of spherical, linear, and spatial charges, such as a coil of a bulk spiral and plane annular coils and Archimedes' spiral of various lengths, exploded in air. In the case of explosion of rings and spirals, a complex wave structure in the form of a sequence of several shock waves is registered near the charges along the spiral axes; a weaker attenuation of shock waves with distance and pressure amplitudes two to three times higher than in the case of a spherical charge of the same mass are observed. It was found that an increase in the length of a plane spiral does not lead to an increase in the maximum pressure in the shock wave at distances of the order of several pitches of the spiral from its plane. With distance from spatial charges of different shape but identical mass, the pressure values in the shock-wave fronts coincide and tend asymptotically to the parameters of a spherical explosion with a significant increase in the duration of a wave packet generated by the spatial charge. Dependences for evaluation of shock-wave pressure amplitudes in the near zone of the explosion are presented.

Introduction. Charges of condensed high explosives (HE), chemically active gas mixtures, and explosive-type sources are used to solve a number of problems in hydroacoustics as powerful sources of sound whose radiation is registered at a significant distance. Antenna-type systems of these sources and spiral-type spatial charges allow one to solve problems related to the direction of radiation and its duration [1, 2]. We note that the latter are formed from the so-called cord charges with which it is possible to solve hydroacoustics problems using these linear charges as continuously distributed sources of explosive sound. Data of long-term studies on shock-wave propagation from linear (and also spherical) charges in various media can be found in [3].

The objective of the present work is to study the wave-field parameters and structure in the case of bulk charges such as rings and plane spirals exploded in air. We define the near zone for spatial charges as the range of distances $0 < r \leqslant 15R_0$ counted from the center (plane) of the charge with a characteristic radius R_0. For the demolition cord (DC) itself from which the spatial charge is formed, the scale of the near zone ($r \leqslant 15r_0$) is determined by its cross-sectional radius r_0.

1. Statement of the Experiments. Experiments with spatial charges and also test experiments with spherical and linear charges were conducted in a spherical explosive chamber 10 m in diameter with a horizontal concrete floor aligned 1 m below its center. A standard DC was used in the experiments. It consisted of RDX of density of 1.6 g/cm^3 with an HE charge diameter of 3 mm and an outer coaxial shell with a 4.8-mm diameter, which was impregnated by water repellent. The specific weight of the HE and inert shell was 11–12 and 11 g/m, respectively, the specific heat of explosion was $Q = 1400$ kcal/kg, and the detonation rate was 7.5 km/sec. The charge was initiated by industrial high-voltage detonators ÉDV-1 and ÉD-637 with a content of secondary HE of approximately 1 and 0.3 g, respectively.

Lavrent'ev Institute of Hydrodynamics, Siberian Division, Russian Academy of Sciences, Novosibirsk 630090. Translated from Prikladnaya Mekhanika i Tekhnicheskaya Fizika, Vol. 41, No. 5, pp. 81–90, September–October, 2000. Original article submitted June 23, 2000.

In test experiments, a linear charge of a DC two to three meters long was suspended horizontally at a height of 1.5 m from the floor and was initiated on one end. Three pressure transducers were located in the central plane perpendicular to the charge axis along circular radii (with a step of 45°). Shock waves (SW) were registered at distances r = 15, 20, 50, and 100 cm from the charge axis. A spherical cast charge of 50/50 TNT/RDX of radius of 12 mm (equivalent to a DC charge 1 m long) was initiated from the center by an ÉD-637 detonator, and the pressure was measured by a piezoelectric transducer at distances r = 10, 15, 30, ..., 150 cm from the charge center. The SW velocity was measured by the time interval of wave registration by two rod piezoelectric transducers (the crystal radius was r_0 = 1 mm) on a base of 15 mm.

Plane annular charges of diameter D_0 = 300, 450, and 600 mm, coils of a bulk spiral with a pitch h = 150 mm, D_0 = 300 mm, and length L = 1 m, coils of a plane spiral with a pitch h = 150 mm, L = 1 m, and charges in the form of a plane Archimedes' spiral (a DC length of 10 m and a pitch of 150 m) were fixed on a rigid cylindrical frame made of steel wire 6 mm in diameter and suspended at a height of 1.5–2.0 m from the floor. The shape of the frame and the method of DC attachment to it allowed us to avoid noticeable distortions of the pressure field due to the waves reflected from the frame. To attenuate the explosive wave from the initiating detonator, the experimental assembly contained a steel thick-walled tube about 1 m long inside of which was a DC sector connecting the charge examined with the detonator. The detonation was excited from the most remote end of the charge from the transducer, and the shock waves were registered by one piezoelectric transducer along the charge axis within the range of relative distances $r^* = r/R_0$ = 1–10 or $r^* = r/h$ = 1–10 counted from the central plane of symmetry (for a bulk coil, the center of symmetry is located at the axis at a distance of 75 mm from the butt-end faces).

The signals of the pressure transducers were consecutively supplied to a source follower with an input voltage of 10^9 Ω and a two-beam digital oscillograph S9-16 whose information was fed to a PC-386 computer. The oscillograph was triggered by a GZI-6 delayed pulse oscillator by a high-voltage (5 or 10 kV) pulse of current used to initiate the detonator.

In the scheme of SW registration, we managed to significantly decrease "spurious" effects, which are associated with excitation of electric signals in cables and joints, which is caused by mechanical loads, and with electromagnetic radiation caused by the action of shock waves on materials used to attach and acoustically separate the transducers. These effects arise in rubber or plastic tubes used for protection against the cable effect under a shock-wave action.

The construction of these rod transducers and the method of pressure measurement were described by Lyamin et al. [4]. In addition, knife transducers with a disk plate 30 mm in diameter were manufactured. The thickness of the central part of this plate was 3.5 mm, and a piezoelectric element 2 mm in diameter and 0.4 mm thick was soldered to the body in the cavity of this plate. The disk plate was fixed on a copper tube 7 mm in diameter and 70 mm long. The eigenfrequency of the transducers was 300–500 kHz. In the experiments described, transducers based on a TsTS-19 ferroelectric are more preferable than tourmaline transducers with a relatively low sensitivity.

2. Results of Test Measurements. In conducting test experiments, the data on linear DC based on which the above-described spatial charges were formed are particularly important. These data and the data on spherical charges were compared with the results obtained in [3, 5, 6]. Transient shock waves in test experiments were measured by knife transducers with the disk plane perpendicular to the wave front. The experimental data on the maximum pressure in transient shock waves coincided with the calculated values for an identical SW velocity. In experiments with an incident SW, where butt-end transducers calibrated in a shock tube were used, the amplitudes were also close to the calculated values for reflected shock waves.

Linear Charge. The experimental pressure profiles in the SW induced by blasting a linear charge are shown in Fig. 1a for $r \approx 20$ cm (for comparison, Fig. 1b shows the pressure profile for a 100-g spherical charge for $r \approx 30$ cm). A typical two-wave structure is seen (the second, weaker SW is registered after approximately 340 μsec behind the front of the primary wave). The characteristic length of the wave τ (the time counted from the SW front to zero pressure difference) increases with distance from the charge. Thus, for r = 150,

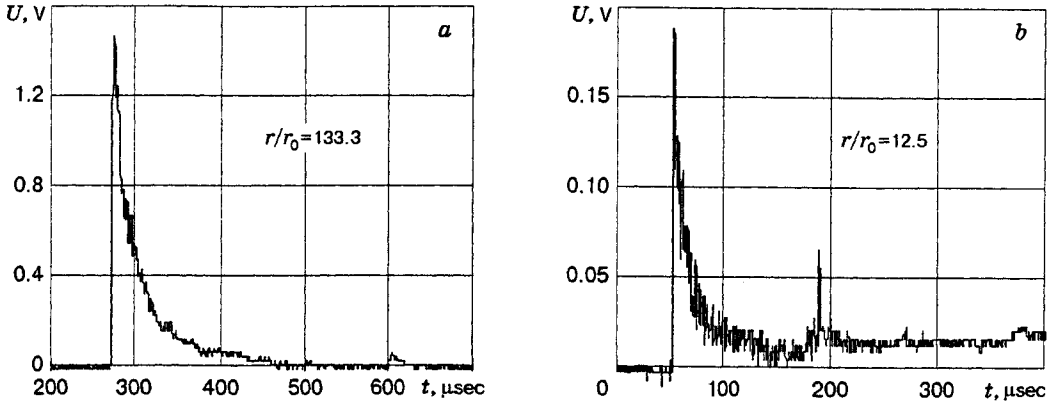

Fig. 1. Experimental pressure profiles obtained by blasting a linear HE charge ($r \approx 20$ cm) (a) and a spherical HE charge ($r \approx 30$ cm) (b).

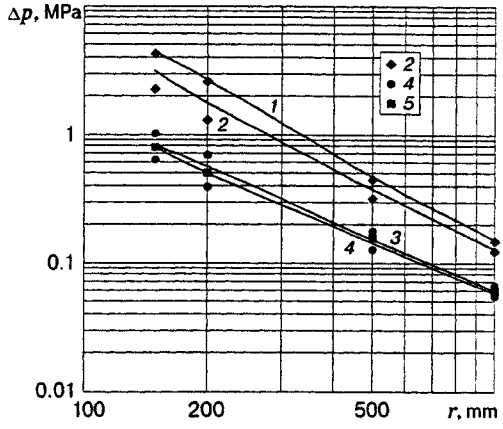

Fig. 2. Decay of shock waves after explosion of linear charges: curves 1 and 3 refer to the calculations for the reflected and transient shock waves, respectively; points 2 and 4 are the experimental data on the pressure in the incident Δp_2 and transient Δp_1 shock waves, respectively; points 5 are the experimental data of [5].

200, 500, and 1000 mm, it varies within the intervals τ = 150–250, 190–280, 350–420, and 500–580 μsec, respectively.

The pressure in the front of the transient SW Δp_1 decreases from 1.02–0.63 to 0.065–0.055 MPa with increasing r within the given range (points in Fig. 2). The experimental curves for the incident SW (curve 2) and transient SW (curve 4) were obtained by averaging the results of ten experiments for each value of r. The greatest scatter in the values of Δp_1 relative to the mean value is $\pm$(25–30)% and is observed near the charge (r = 150 and 200 mm) both in one test for different transducers and in different tests for one transducer for the same value of r. The corresponding root-mean-square deviation is 10–13%. For r = 1 m, the scatter in the values of Δp_1 decreases to $\pm$(5–7)% and almost coincides with the measurement error (less than 5%). Obviously, at the stage of expansion of explosion products, the inhomogeneous character of failure of the inert shell has a significant effect on SW formation and parameters, which is confirmed by the analysis of oscillograms (pressure oscillations in the front and wave profile).

Attenuation of the shock wave by the charge shell was mentioned in [5, 7], though the instability and scatter of SW parameters from one experiment on DC explosion to another were not reported in these papers. Tsykulin [5] found that, in the case of an inert shell with a specific weight of 19 g/m and HE (RDX) with a specific weight of 14.2 g/s, the pressure in the SW front in the near zone decreases by a factor of 2.5 and the impulse (in the compression phase) decreases by a factor of 1.8 as compared to an explosion of an identical HE

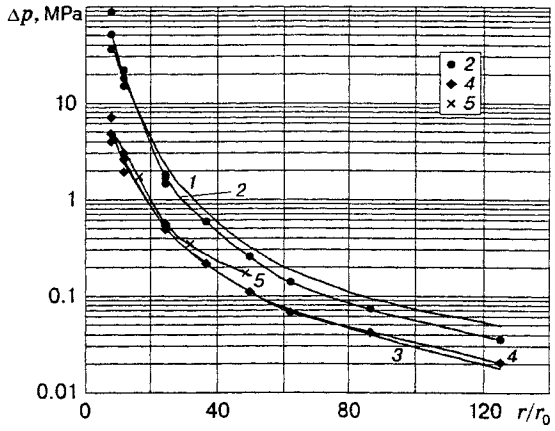

Fig. 3. Decay of shock waves after blasting spherical charges: curves 1 and 3 refer to the calculation for the reflected and transient shock waves, respectively, points 2 and 4 are the experimental data on pressure in the incident (Δp_2) and transient (Δp_1) shock waves, respectively, points 5 are the experimental data of [7].

charge without the shell. For detonation of a short section of the PETN DC, Vasil'ev and Zhdan [7] registered in schlieren pictures a significant (by a factor of 1.5–2) decrease in the SW front velocity as compared to the calculation with the shell effect ignored at distances up to $50r_0$ from the charge.

The pressure jumps in the front of the transient SW $\Delta p_{1,\mathrm{calc}}$ (curve 3 in Fig. 2) calculated by the mean SW velocity D and the experimental data $\Delta p_{1,\mathrm{exp}}$ (curve 4 in Fig. 2) almost coincide within the entire measurement region with the experimental data of [5] and may be approximated by the relation

$$\pi_1 = bx^{-a}, \tag{1}$$

where $a = 1.372$. If $\pi_1 = \Delta p_1$ and is measured in megapascals and x is measured in meters, then we have $b = 5.655 \cdot 10^{-2}$. For $\pi_1 = \Delta p_1/p_0$ and $x = r/r_0$, we obtain $b = 4240.1$. If we introduce the characteristic size for a cylindrical charge $\lambda = (q_l/p_0)^{0.5}$ [5] ($q_l = Qm/L$ is the explosion heat per unit length of the charge and $m/L = 11.5$ g/m is the specific weight of the charge), then we have $\lambda = 0.82$ m. For $\pi_1 = \Delta p_1/p_0$ and $x = r/\lambda$, we obtain $b = 0.743$.

Spherical Charge. By similar measurements, the scatter in the values of Δp_1 in the SW front at distances $r = 0.1$ and 0.15 m was obtained for a spherical charge; it was of the same order as for a linear charge. This indicates the presence of instability of the boundary of expanding products and the manifestation of instability at the early stage for SW formation even in the absence of the inert shell. For $r > 0.3$ m, the scatter in Δp_1 does not exceed the measurement error. The experimental results of pressure measurements by knife and butt-end transducers and the calculated values of the pressure difference versus the velocity of the transient and incident shock waves are plotted in Fig. 3. The relative pressure difference $\Delta p_1/p_0$ in the transient SW as a function of r/r_0 within the entire range of measurements is described by relation (1) with $a = 2.039$ and $b = 3.56 \cdot 10^3$.

The calibration coefficients of butt-end piezoelectric transducers for the linear and spherical cases coincide within the measurement error and allow one to determine the pressure in the SW with an error of less than 5%. Figure 4 shows the measured SW velocity D as a function of r for spherical and linear charges. The measurement error of D is about 3%. The greatest scatter is observed near the charge; it coincides with the scatter in Δp_1 within the entire measurement region.

3. Annular and Spiral Charges. We note that knife transducers are not very effective in the near zone for registration of shock waves induced by blasting spatial charges because of the spatial character of the flow: they distort the flow. As a result, reflected waves and a "shadow" region for the piezocrystal appear. In the experiments with spatial charges described, the pressure in the SW was measured along the axis by butt-end piezoelectric transducers, which distort the flow to a smaller extent. For spatial charges,

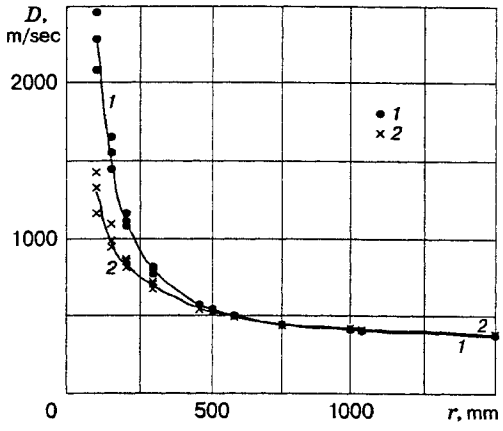

Fig. 4. SW velocity versus distance during explosion of spherical (1) and linear (2) charges.

TABLE 1

Charge shape	τ, μsec						
	$r^* = 1$	$r^* = 2$	$r^* = 3$	$r^* = 4$	$r^* = 5$	$r^* = 7$	$r^* = 10$
Ring	110–125	140–150	190–290	280–290	320–370	465–475	650
Bulk coil	80–105	120–140	170–190	240–270	305–320	440–475	680–700
Plane coil	60–95	140–170	140–190	195–230	340	385	550–650

the pressure difference in transient shock waves $\Delta p_1 = p_1 - p_0$ was determined using the calibration curves $\Delta p_1 = k\Delta p_{2,\text{exp}}$ obtained in test measurements (calibration in the incident wave).

At the first stage of experiments, charges of the same mass but different shape were compared. The pressure profiles were similar for all three types of charges. The characteristic pressure oscillograms for different relative distances r^* are plotted in Fig. 5 for DC charges with $L = 1$ m. A two-wave structure is observed in the near zone ($r^* = 1$). The amplitude of the second wave can be greater than the amplitude of the first one by a factor of 1.5 to 2 for a ring (Fig. 5a) and a bulk spiral (Fig. 5b) and by a factor of 6 to 7 for a plane spiral. Origination of the first wave is related to exploding of the charge end closest to the transducer, and origination of the second wave with focusing of a curved SW converging in the inner region of the charge. At a greater distance from the charge, the bow shock wave has a smoothly decreasing triangular profile (oscillograms on the right of Fig. 5a–c). The wave duration τ for the charge shapes considered almost coincide for identical r^*, and their value changes almost linearly from 60–125 to 650–700 μsec with increasing r^* from 1 to 10 (see Table 1).

For all spatial charges, the scatter in pressure relative to the mean value in the near zone reached ±(25–30)% (the root-mean-square deviation was 10–15%) and decreased in the far zone to ±(5–8)%. Figure 6 shows the experimental data on the decay of the first and second waves [the dependences $\Delta p(r^*)$]. The pressure in the SW front for three types of charges almost coincide beginning from $r^* \geqslant 3$ and does not depend on the shape of the spatial charge (curves 1–3). The SW amplitude in this region is described by relation (1) with $a = 2.31$ and $b = 48.6$.

A comparison of experimental data for spatial (curves 1–3 in Fig. 6) and spherical charges of an equivalent HE mass (curve 4 in Fig. 6) shows that spatial charges yield a gain in the pressure magnitude by a factor of 2 to 3 as compared to those concentrated at identical absolute distances from the geometric center of the charge. This is related to a sharper decrease in pressure in the SW front in the spherical case ($p \sim r_f^{-1.5}$) as compared, for example, to the cylindrical case ($p \sim r_f^{-1}$) [8], where an additional effect of radiation directivity in the plane perpendicular to the charge axis is manifested. Note that, among all types of spatial charges considered, the best directed and focusing action along the axis (in the zone nearest to the charge) is exerted by a bulk coil of a spiral in which the pressure in the second-wave front reaches 6.5 MPa for $r^* = 1$.

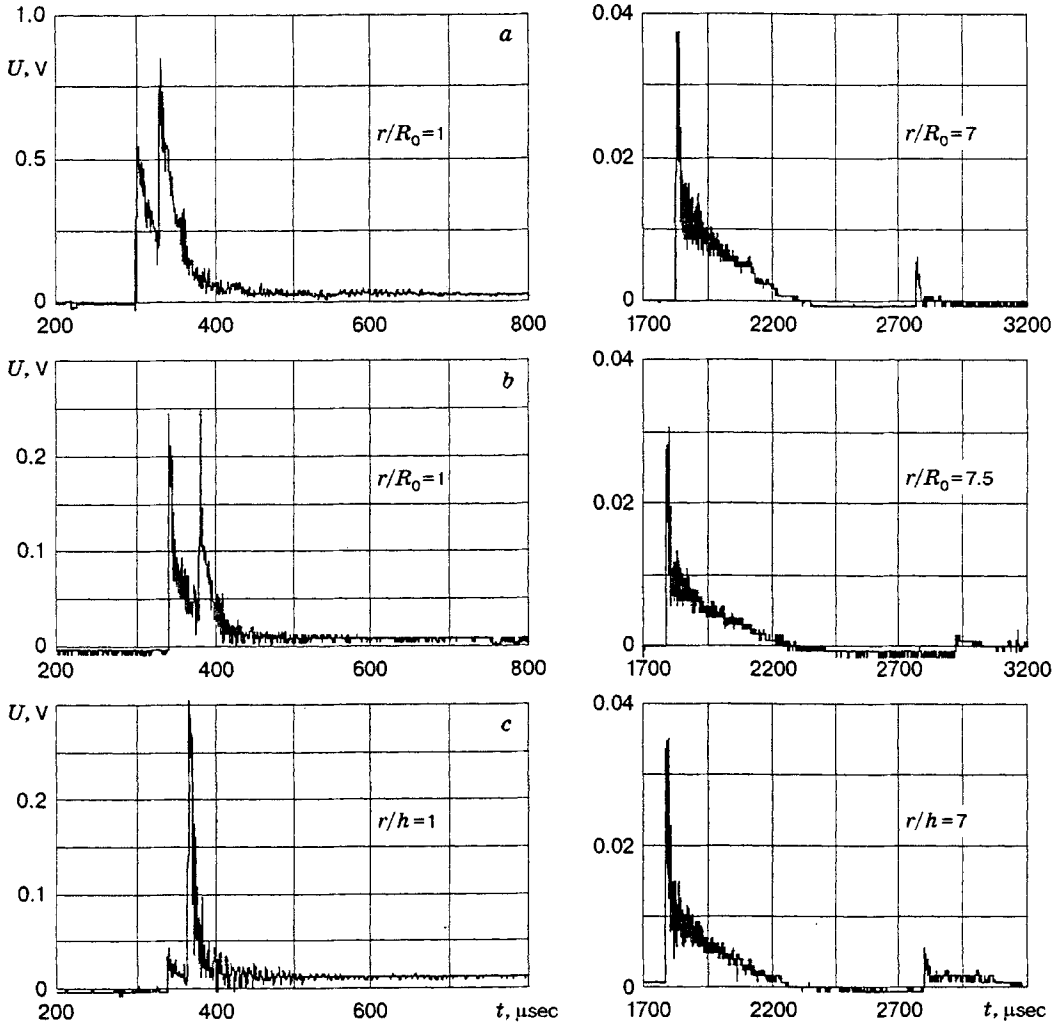

Fig. 5. Typical oscillograms of pressure along the axes after explosion of DC charges 1 m long in the form of rings (R_0 = 150 mm) (a), a coil of a bulk spiral (R_0 = 150 mm and h = 150 mm) (b), and a plane spiral (h = 150 mm) (c).

It is of interest to consider the structure of the wave field arising as a result of explosion of a multicoil plane spiral (plane Archimedes' spiral with a DC length of 10 m and a pitch of 15 cm) at different distances along the axis. Its dynamics is shown in Fig. 7a–c in the form of pressure oscillograms with scanning times of 2, 4, and 8 msec, respectively. The DC detonation was initiated from the external coil. The spiral "radiation" is a wave packet of a complex structure, which is characterized by an obvious inhomogeneity of the pressure field in terms of amplitude. The oscillogram in Fig. 7a corresponds to a distance of 15 cm from the spiral plane, i.e., it is equal to the spiral pitch h. For $t \approx 1600$ μsec, a strong wave is registered, and its amplitude is an order of magnitude greater than the other perturbations in the wave packet. With distance from the charge and decreasing mean amplitude, a finer structure of the packet can be observed (Fig. 7b), though optical filming data are necessary to identify parts of the spiral or zones of focusing that generate the corresponding waves in the packet. The experiment shows that the duration of the wave packet generated in the case of blasting a spiral charge can be significantly greater than the time necessary for the detonation wave to cover the DC length in the charge (Fig. 7c). This "extension" of the signal is, obviously, related to focusing times.

Though the analysis of the structure is complicated by the strong dependence of the SW velocity in air on the distance to the charge (in contrast to hydroacoustics), some special features are worth noting. Figure 8

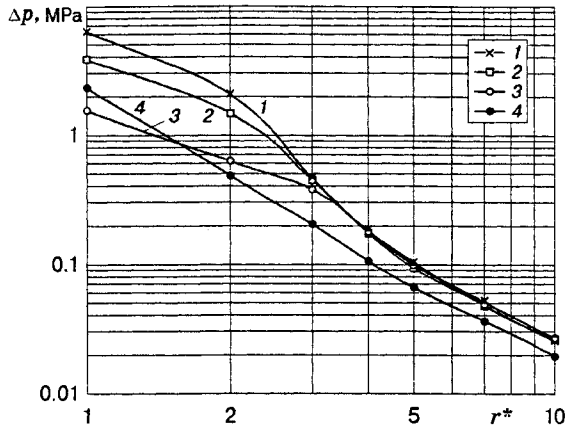

Fig. 6. Decay of pressure in the front of transient shock waves for charges of an identical mass in the form of a bulk coil (1), a coil of a plane Archimedes' spiral (2), a plane ring (3), and a sphere (4).

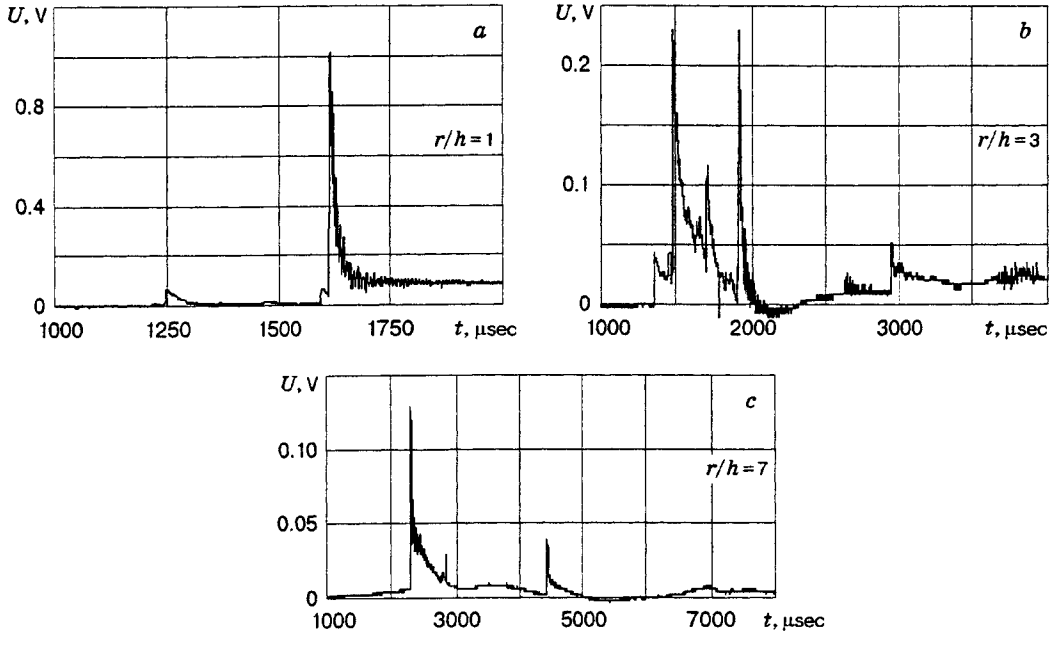

Fig. 7. Typical pressure oscillograms for a plane Archimedes' spiral ($h = 150$ mm and $L = 10$ m) for scanning times of 2 (a), 4 (b), and 8 msec (c).

shows the experimental data on the distribution of pressure amplitudes in wave packets generated by blasting charges in the form of a plane coil and Archimedes' spiral. The curves are approximations of experimental data (points). For comparatively small distances $r^* = 1$ (Fig. 7a), the greatest amplitude in the wave packet with a total (resolvable) duration $\tau \geqslant 750$ μsec is reached in the third or fourth wave (curve 1 in Fig. 8). The amplitude of the first SW (curve 2) is lower by almost an order of magnitude. In the intermediate region $2 < r^* < 5$, several waves with close amplitudes of pressure ($\tau \approx 650$–750 μsec) are observed, since the effect of external coils of the spiral becomes more noticeable with distance from the charge plane (see Fig. 7). For $r^* > 5$, as a result of merging of a series of shock waves (curves 1 and 2 coincide in Fig. 8), a bow SW is formed ($\tau \approx 700$–750 μsec), which is followed by a second, weaker SW approximately 2.1 msec later (see Fig. 7c).

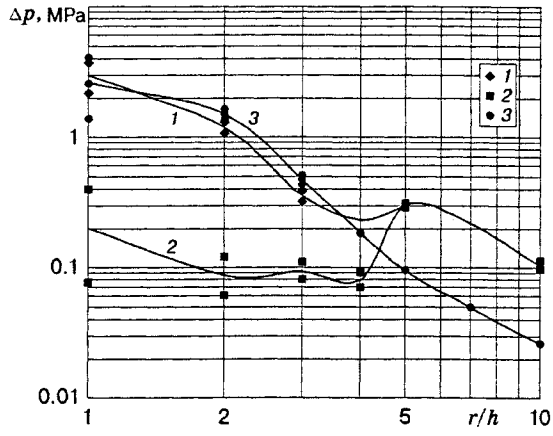

Fig. 8. SW decay in the case of blasting a plane coil and Archimedes' spiral: 1) pressure $\Delta p_{3,4}$ in the third or fourth wave with the greatest amplitude in the case of explosion of an Archimedes' spiral; 2) pressure Δp_1 in the bow SW of the same charge; 3) pressure Δp_1 in the case of blasting a plane coil.

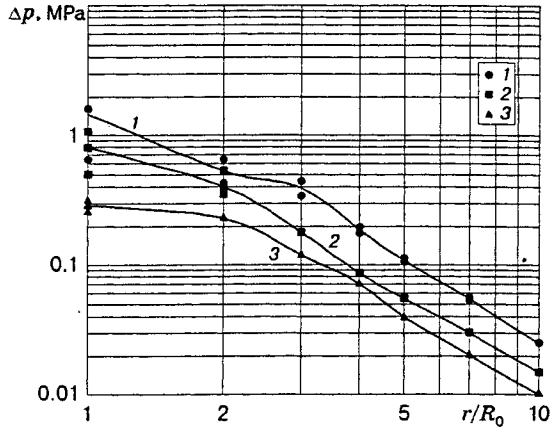

Fig. 9. Decay of an SW induced by blasting plane rings of different radius along their axes for R_0 = 150 (1), 225 (2), and 300 mm (3).

The experimental dependences $\Delta p(r/h)$ in the SW in the case of blasting a coil and a plane spiral (curves 3 and 1 in Fig. 8, respectively) show that the spiral length in the zone closest to the charge has practically no effect on the maximum pressures in the SW, which are rather close for both charges. For $r^* > 4$–5, the situation becomes dramatically different: the wave amplitudes in the packet induced by explosion of the spiral are significantly greater than the wave amplitudes in the packet generated by explosion of a single coil. Naturally, the wave duration and its total impulse increase. A comparison of the pressure oscillogram in Figs. 5c and 7 allow us to conclude that weaker shock waves with gradually increasing values of pressure in the SW front are formed by external coils of a large radius with detonation propagating to the center along these coils, and the maximum pressure amplitude in the last shock wave is reached due to the focusing of a curved shock wave generated by explosion of a coil of the central part of a plane spiral approximately 1 m long.

This effect is more pronounced in experiments with three annular charges with radii R_0 = 150, 225, and 300 mm. The results of these experiments are plotted in Fig. 9 [the curves are approximations of experimental data (points)]. As the radius of an individual ring (or a specified coil of a plane Archimedes' spiral) increases, the pressure in the shock wave in the near zone at a fixed distance decreases. The results obtained on the shock-wave amplitude for DC rings can be described by empirical formulas. For a ring with R_0 = 150 mm,

we have

$$\pi_1 = 0.081x^3 + 0.164x^2 - 1.057x + 2.25 \quad \text{for} \quad 1 \leqslant x \leqslant 4,$$

$$\pi_1 = 3.674x^{-2.17} \quad \text{for} \quad 4 \leqslant x \leqslant 10.$$

Here π_1 is measured in megapascals and $x = x'/R_0$ (x' is the distance from the charge plane in millimeters).

4. Conclusions. The experimental studies show that the considerable scatter in data on pressure and SW velocities registered in the near zone in the case of blasting spatial, spherical, and cylindrical charges in air is caused by the instability of the boundary of expanding detonation products. It was experimentally found that the SW induced by blasting spatial charges decays more weakly and the amplitudes in the SW front are two to three times higher as compared to spherical charges of the same mass. As the point of registration moves away from spatial charges of identical mass (rings and spiral coils), the pressure in the SW front tends asymptotically to a value corresponding to a concentrated charge of an equivalent mass.

The main features of spatial charges are the directed radiation, the greater SW amplitude as compared to concentrated charges of the same mass in the near zone wherein the effect of mass equivalence is not manifested, and the radiation duration, which is orders of magnitude greater as compared to concentrated charges of the same mass. As the DC length increases, the duration (approaching 3 msec for a DC length of about 10 m) and impulse of the wave packet in a plane spiral increase without significant increase in pressure in shock waves in the near zone from the spiral plane (at distances from one to several pitches of the spiral). The greatest jump in the SW is observed in the case of focusing of a curved shock wave in the central region of the charge.

REFERENCES

1. V. K. Kedrinskii, "Underwater explosives sound sources," in: M. J. Crocker (ed.), *Encyclopedia of Acoustics*, Vol. 1, John Wiley and Sons, New York–Toronto (1997), pp. 539–547.
2. V. K. Kedrinskii, "Special features of the shock-wave structure at underwater explosions of spiral charges," *Prikl. Mekh. Tekh. Fiz.*, No. 5, 51–59 (1980).
3. *Mechanical Action of Explosion* (collected scientific papers) [in Russian], Inst. of Dynamics of Geospheres, Russ. Acad. of Sci., Moscow (1994).
4. G. A. Lyamin, A. V. Pinaev, and A. S. Lebedev, "Piezoelectrics for measurement of impulsive and static pressures," *Fiz. Goreniya Vzryva*, **27**, No. 3, 94–103 (1991).
5. M. A. Tsykulin, "Air shock wave in explosion of a cylindrical charge of large length," *Prikl. Mekh. Tekh. Fiz.*, No. 3, 188–193 (1960).
6. V. V. Adushkin, "Formation of a shock wave and spreading of explosion products in air," *Prikl. Mekh. Tekh. Fiz.* No. 5, 107–114 (1963).
7. A. A. Vasil'ev and S. A. Zhdan, "Shock-wave parameters on explosion of a cylindrical charge in air," *Fiz. Goreniya Vzryva*, **17**, No. 6, 99–105 (1981).
8. L. I. Sedov, *Similarity and Dimensional Analysis*, Academic Press, New York (1959).